Polypropylene/Silica Nanocomposites Prepared by in-Situ Sol−Gel Reaction with the Aid of CO_2

Donghai Sun, Rui Zhang, Zhimin Liu, Ying Huang, Yong Wang, Jun He, Buxing Han,* and Guanying Yang

Center for Molecular Sciences, Institute of Chemistry, The Chinese Academy of Sciences, Beijing 100080, China

Received December 27, 2004; Revised Manuscript Received April 23, 2005

ABSTRACT: Polypropylene/silica (PP/Silica) composites were prepared by two steps: tetraethyl orthosilicate (TEOS) was first impregnated into PP matrix using supercritical carbon dioxide (SC CO_2) as a swelling agent and carrier followed by hydrolysis/condensation reaction of TEOS confined in polymer network. The effects of soaking temperature, CO_2 density, and initial TEOS concentration on the mass uptake of TEOS in PP were investigated. Hybrids with high silica load could be achieved by repeating the steps. The hybrids were characterized by attenuated total reflectance infrared (ATR-IR), ^{29}Si solid-state nuclear magnetic resonance spectroscopy (^{29}Si solid-state NMR), thermal gravimetric analysis (TGA), transmission electron microscope (TEM), scanning electron microscopy (SEM), and mechanical testing. The results showed that nanosized silica networks were formed and distributed uniformly in PP matrix, and some polymer molecules might entangle with the silica networks. The PP/Silica composites had much higher tensile strength and Young's modulus than virgin PP due to their special morphology.

Introduction

Exploitation of hybrid organic−inorganic composites has received much attention for their scientific interests and industrial applications.[1−3] These hybrid composites with organic and inorganic moieties mixed on a molecular scale may achieve a synergetic combination of the properties which cannot be obtained by each of the component. Extensive studies have been devoted to the hybrid of polymer-layered silicate nanocomposites. The pioneer work of Toyota researchers showed that introducing a few weight percent of modified clay nanofillers into nylon matrix resulted in drastic increases in heat-distortion temperature, modulus, tensile strength, and yield stress.[4,5] This method can be used to modify high surface energy polymers such as polyamides, where polarity and hydrogen-bonding capacity generate enough adhesion between the organic and inorganic phase. However, it is difficult to synthesize polyolefin nanocomposites because these low-energy materials interact only weakly with clay surfaces. The successful synthesis of these nanocomposites requires the use of expensive maleated polyolefin and surfactant-intercalated clays to overcome the incompatibility between polymer and clays.[6−8] Furthermore, limited improvement of tensile modulus vs virgin polymer was achieved.[9] Efforts of in-situ polymerization with metallocene/clay catalysts were also made.[10−14] However, this method often suffers low catalyst efficiency, low molecular weight of the resulting polymer, and limited improvement of mechanical properties.

Another extensively used approach for preparing organic−inorganic hybrids is the sol−gel technique,[15] which allows the formation of metal oxide frameworks starting from molecular precursors at ambient temperature. Hybrid systems prepared by the sol−gel process can be obtained using different synthetic approaches. The most common one is polymerization of alkoxysilanes in the presence of preformed organic polymers.[16−18] The composites were usually synthesized by codissolving a precursor, usually a tetrafunctional metal alkoxide, with polymer in a common solvent. The subsequent hydrolysis and condensation reaction of the inorganic precursor result in the formation of inorganic phase in polymer network. This method is especially interesting because it can be used to directly modify commercially available polymers.

An obvious problem associated with the sol−gel process is the use of organic solvent, which must be removed from the final product. Difficulties often come from the limited choice of solvents that can simultaneously dissolve both inorganic precursors and organic polymers. Though many polymers have been successfully incorporated with inorganic component by different synthetic approaches,[2] hybrids with extensively used polyolefin, like polypropylene and polyethylene, have not been prepared for their poor solubility in common solvents and their high crystallinity.

In recent years, there has been great interest in the application of SC CO_2 to polymer processing.[19−23] The motivation of using SC CO_2 stems not only from the fact that it can replace many environmentally harmful solvents but also from the opportunity to utilize their unique properties for preparing new polymeric materials. SC CO_2 can effectively swell and plasticize the amorphous region of the polymers and leave the polymer just by release of pressure. Small molecules dissolved in SC CO_2 can be infused and deposited into a polymer matrix exposed to such a solution. Extensive studies have been carried out on impregnation of reactive monomers into the polymers. Subsequent polymerization leads to the formation of polymer composites[24−34] or modification of polymer backbone.[35−41] Recently, several papers have reported CO_2-assisted fabrication of inorganic/polymer hybrid materials in SC CO_2.[42,43] Lesser et al. developed a synthetic route to polymer-based composites with high concentration of clay and a high degree of order.[42] Green and co-workers cross-linked poly(styrene-*co*-allyl alcohol) (PSAA) or soluble starch (SS) by infusing $SiCl_4$ into them using SC CO_2 as the carrier medium.[43] Zeng et al. prepared polymer−

10.1021/ma047314h CCC: $30.25
Published on Web 05/17/2005

clay nanocomposites foams using SC CO_2 as the foaming agent.[44]

In this article, we describe the preparation of PP/silica composites using a two-step route. In the experiments TEOS was first impregnated into PP films with the aid of SC CO_2, and then the composite was prepared by hydrolysis/condensation reaction of the films in acidic water. The hybrids were characterized by various techniques.

Experimental Section

Materials. The polypropylene (240, Yanshan Petrochemical Co. Ltd., Beijing, China) was hot pressed into 100 μm thin films at 200 °C. The samples were annealed in ice water after compression molding and the crystallinty determined by DSC was 44.5%. CO_2 with a purity of 99.95% was supplied by Beijing Analytical Instrument Factory and used as received. Tetraethyl orthosilicate (TEOS, AR) was supplied by Beijing Chemical Reagent Co.

Composite Synthesis. The composites were prepared by two successive steps: impregnation of PP films with TEOS in SC CO_2 and hydrolysis/condensation reaction of TEOS confined within PP in acidic aqueous solution. The impregnation of the PP films was performed in a 22 mL high-pressure stainless steel vessel. In a typical experiment, the vessel was charged with TEOS and PP films (~0.2 g) and purged with CO_2. Suitable CO_2 was charged into the vessel using a high-pressure metering pump at suitable temperature. After desired soaking period, the pressure was released into the hood slowly. The samples were washed with ethanol to remove the TEOS adsorbed on the surface of the PP films. The experiments demonstrated that the mass of the samples was constant after 24 h after releasing CO_2, indicating that all the CO_2 absorbed in polymer films escaped from the matrix. In all the experiments, the mass uptakes were determined after the mass of the films became constant. The mass uptake of PP film in this process was calculated from the following equation

$$\text{mass uptake (wt \%)} = 100 \times (W_1 - W_0)/W_0$$

where W_0 and W_1 stand for the masses of original PP film and that of the sample after impregnation.

The hydrolysis/condensation reactions of incorporated TEOS were carried out on sheets embedded in acidic water (HCl, 1 M) at 80 °C according to the process adopted by Michel.[45] To achieve high silica uptake, some composites were fabricated via repeating the above steps several times.

Characterization. Transmission and attenuated total reflectance (ATR) infrared spectroscopic experiments were conducted using a Bruker Tensor 27 FTIR. Thermal gravimetric analysis (TGA) was carried out with a DuPont Instruments TGA 2950 at a heating rate of 10 °C/min from room temperature to 600 °C in an air atmosphere. Differential scanning calorimetry (DSC) was conducted on a Perkin-Elmer DSC-7. About 4 mg of the sample was heated to 220 °C at a heating rate of 20 °C/min. ^{29}Si solid-state NMR spectra were recorded on a Bruker MSL-400 NMR spectrometer, using a standard double air-bearing cross-polarization/magic angle-spinning probe, operated at a frequency of 79.5 MHz for ^{29}Si. Samples were loaded into 4 mm fused zirconia and sealed with Kel-FTM caps. The spinning rate was 4700 Hz. Scanning electron microscopy (SEM) was used to study the structure and morphology of the hybrid material. The SEM samples were prepared by breaking the composites in liquid N_2 and coated with Pt before the examination. A Hitachi S-800 scanning electron microscope attached with energy-dispersive X-ray (EDAX DX4) microanalysis equipment was used to determine elemental composition of the samples. TEM micrographs were taken on a Philips CM100 transmission electron microscope. Ultrathin sections were microtomed from the film. The mechanical tensile properties of the films were determined with an Instron model 3365. A high-compression stamp was used to produce samples of constant length and width of 3 cm and 0.4 cm, respectively. The cross-head speed was held at 10 mm/min, and all samples were tested at 25 °C and 50% relative humidity. At least five tests were averaged for each sample.

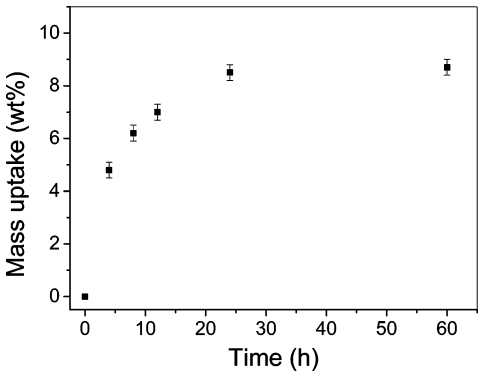

Figure 1. Effect of soaking time on mass uptake. TEOS concentration is 0.15 mol/L; CO_2 density is 11.14 mol/L; soaking temperature is 80 °C.

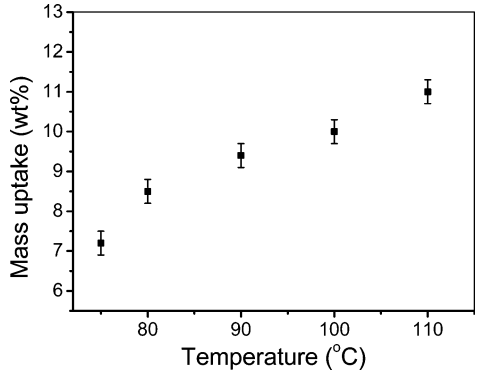

Figure 2. Effect of soaking temperature on mass uptake. TEOS concentration is 0.15 mol/L; CO_2 density is 11.14 mol/L; soaking time is 24 h.

Results and Discussion

Impregnation of PP with TEOS. To prepare the composites, the PP films were first impregnated with TEOS using SC CO_2. The effects of various parameters such as the soaking temperature, soaking time, CO_2 density, and the concentrations of TEOS on mass uptake were studied.

Figure 1 shows the mass uptake at different soaking time at 80 °C, and the TEOS concentration and CO_2 density are 0.15 mol/L and 11.14 mol/L, respectively. The figure indicates that the mass uptake increases initially with soaking time and is independent of soaking time after about 24 h; i.e., equilibrium can be reached in about 24 h. A soaking time of 24 h is used in the following studies.

Figure 2 shows the effect of soaking temperatures on the mass uptake. The TEOS concentration and CO_2 density are 0.15 mol/L and 11.14 mol/L, respectively. It reveals that the mass uptake increases slightly with increasing soaking temperature. It is known that SC CO_2 can effectively swell and plasticize the amorphous region of polymer materials, which increases the free volume of the polymer matrix. Increase in temperature also induces swelling of the polymers, which is favorable to the absorption of TEOS because larger free volume is favorable to taking more solute molecules.

The effect of CO_2 density on the mass uptake is shown in Figure 3. The mass uptake of TEOS increases to a maximum and then decreases with increasing CO_2

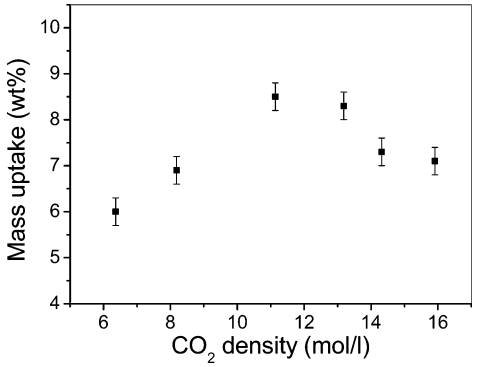

Figure 3. Mass uptake as a function of CO_2 density. Soaking time is 24 h; other conditions are the same as those in Figure 1.

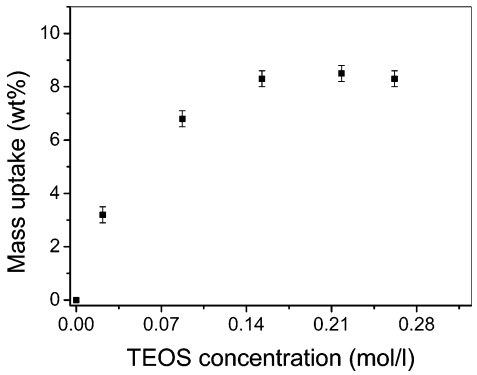

Figure 4. Mass uptake as a function of TEOS concentration. Soaking time is 24 h; other conditions are the same as those in Figure 1.

density. During the soaking process, TEOS distributes between CO_2 phase and polymer phase. Higher CO_2 density results in severer swelling of the polymer, which is favorable to increasing the uptake. However, the increase of the free volume must be ultimately limited by the restriction of the rigid crystalline phase.[25,29] On the other hand, the solvent power of CO_2 is stronger at higher pressure, which is not favorable to increasing the uptake because TEOS tends to exist in CO_2 phase. Therefore, the mass uptake of TEOS decreases with CO_2 density after the pressure is high enough.

The soaking experiments were also conducted at various TEOS concentrations at 80 °C, and the density of CO_2 was 11.14 mol/L (Figure 4). The mass uptake increases initially with increasing TEOS concentration and tends to level off as TEOS concentration is higher than 0.15 mol/L, suggesting that the polymer matrix is saturated as the concentration of TEOS in CO_2 phase reaches 0.15 mol/L.

As seen from the results above, high TEOS uptake may be obtained at high soaking temperature. However, this results in harsh experiment conditions because the effect of temperature on TEOS mass uptake is not pronounced. To increase the silica load, we repeated the impregnation process using the composites, which were obtained after the impregnation/hydrolysis (in 1 M HCl at 80 °C for 3 days) processes, as the matrix, and the results are shown in Figure 5. The figure shows that TEOS can be deposited into PP in each hybridization cycles. The amount of TEOS impregnated into PP each circle decreases slightly with impregnation cycles. As mentioned above, TEOS is deposited in the amorphous region swelled by SC CO_2. The mass uptake in each cycle decreases with cycle mainly because the free

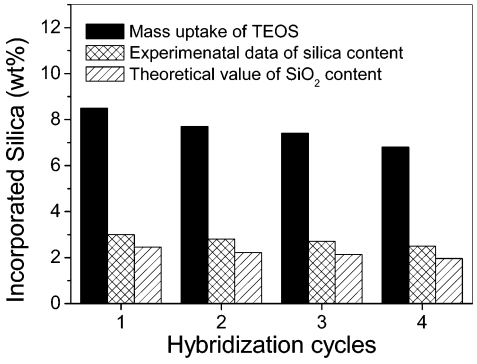

Figure 5. Mass uptake of TEOS at each hybridization cycle. The soaking time of each cycle is 24 h. Other conditions are the same as those shown in Figure 1. The experimental data of silica content were obtained from TGA. The theoretical value of silica content was calculated from the mass uptake of TEOS.

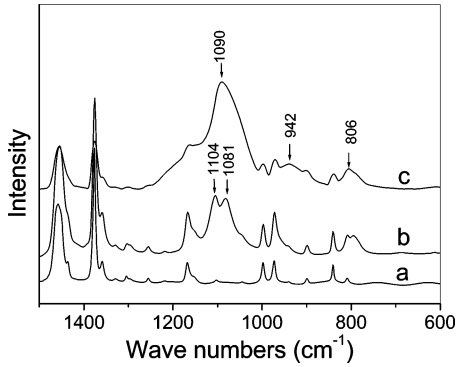

Figure 6. ATR-IR spectra of (a) PP, (b) PP impregnated with TEOS before hydrolysis, and (c) PP impregnated with TEOS after hydrolysis. The curves are displaced vertically to avoid overlap.

volume available for the subsequent impregnation of TEOS is reduced.

Characterization. The PP film and a piece of film impregnated with TEOS before and after hydrolysis were subjected to ATR-IR analysis (Figure 6). Compared with the spectrum of virgin PP, the doublet at 1104, 1081 cm^{-1} due to Si−O−C stretching vibrations[46] appears after impregnation. After hydrolysis in 1 M HCl at 80 °C for 3 days, a strong absorption band in the range 1000−1200 cm^{-1} is observed in the hybrid and is ascribed to asymmetric stretching vibrations of the Si−O−Si bonds of the silica component.[47,48] The asymmetric shape of this peak may result from the different substructures between Si−O−Si groups, e.g., linear and cyclic (1063 and 1108 cm^{-1}).[49] The weak absorbance at 806 cm^{-1} is due to the symmetric Si−O−Si stretching vibration.[49] The absorbance at 942 cm^{-1} is ascribed to the −Si−OH vibration,[50] the presence of which indicates the existence of the unreacted silanol group. All results above indicate the hydrolysis and condensation of TEOS confined in PP matrix and different types of Si−O−Si groups may exist in the system. The existence of the Si−OH group indicates that the condensation reaction was not completely finished.

It is known that ATR-IR spectra assess only the outmost 1−2 μm layer of the sample instead of the whole thickness of the film. On the other hand, transmission IR analysis evaluates the bulk composition of the film. Comparison of the ATR-IR and transmission IR was usually used to determine the structural difference between the surface and bulk.[36,39] Unfortunately, this method was tested to be invalid in analysis of the

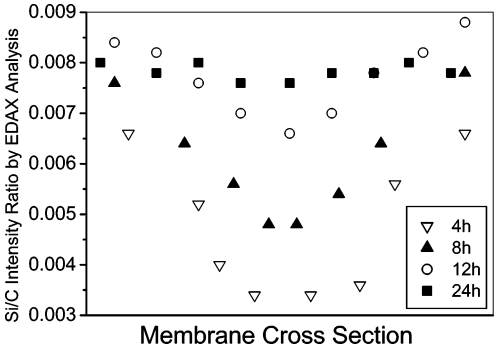

Figure 7. Typical Si/C composition profiles for the samples with different soaking times. The left and right end points of the horizontal axis correspond to the film surfaces.

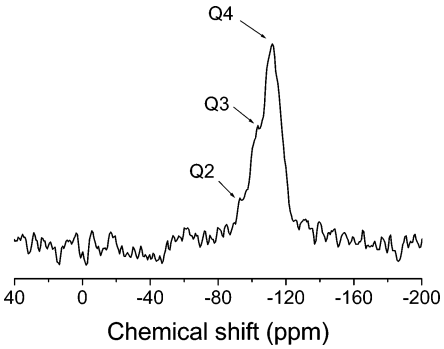

Figure 8. ^{29}Si solid-state NMR spectrum of hybrid with silica content of 11.0%.

composite because the film we used is too thick to get a transmission IR spectrum with satisfactory resolution. We tentatively used SEM-EDAX to determine the homogeneity throughout the film. The integrated intensity of the carbon (C) peak in the EDAX spectrum is adopted as a reference for the polymer matrix. Therefore, the Si/C intensity ratio is taken as a relative measure of local silica content. Figure 7 shows four typical composition profiles with different soaking time. The curves are rather symmetrical about the film center plane. The figure shows U-shape profiles at relatively short soaking time with more silica in the immediate subsurface regions than any other location, especially the middle of the film. However, the negative gradient of this quantity toward the center become less sharp with increasing soaking time. With soaking time longer than 24 h, the difference of Si/C ratio in the profile turns to be negligible, indicating the impregnation equilibrium was reached, which agrees well with the conclusion obtained from dependence of TEOS mass uptake on soaking time shown in Figure 1.

While ATR-IR results show the formation of Si−O−Si groups in the PP matrix, the ^{29}Si solid-state NMR spectra were used to further study the degree of molecular connectivity of the silicate phase. In the ^{29}Si solid-state NMR spectra, peaks are generally denoted by the symbol Qn to show un-, momo-, di-, tri-, and tetra-substituted siloxanes [$(RO)_{4-n}Si(OSi)_n$, R = H or an alkyl group]. The range of chemical shift (relative to tetramethylsilane) of Qn are about −68 to −83, −74 to −93, −91 to −101, and −106 to −120 ppm from 1 to 4, respectively.[51] The degree of condensation within the SiO_2 particles can be evaluated from the Q4 percent. Figure 8 shows the ^{29}Si solid-state NMR spectra of the hybrid with silica content of 11.0%. The main peak appears at −111 ppm adjacent with a minor peak at

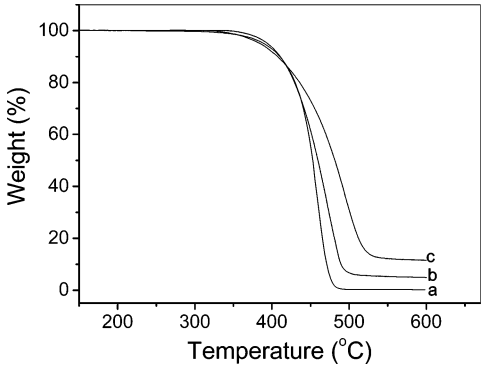

Figure 9. TGA curves of PP (a); hybrids with silica content of 4.7% (b) and 11.0% (c).

−101 ppm, which are Q4 and Q3, respectively. The strong Q4 indicates that the degree of silicon condensation is very high. A weak peak at −92 ppm, which is assigned to Q2, is also observed in the spectrum. The existence of Q3 and Q2 reflects the incomplete condensation of the TEOS.

The actual content of silica in the hydrolyzed hybrid samples was also estimated by TGA analysis. As most polymers are essentially pyrolyzed at about 600 °C, while the inorganic component remains thermally stable at this temperature, the residue left should reflect the actual silica content. The TGA curves show, as illustrated in Figure 9, that the residue of the samples increases with hybridization cycle. The results obtained from TGA are shown in Figure 5. The theoretical silica contents of the samples calculated from the mass uptakes of TEOS in PP by supposing complete hydrolysis/condensation are also shown in Figure 5. The experimental data from TGA are a little higher than the theoretical values. This discrepancy mainly comes from the incomplete hydrolysis of TEOS[49] as proved by ^{29}Si solid-state NMR analysis in this work.

Scanning electron microscopy was used to study the morphology of the hybrid residue from the TGA. Figure 10 shows the SEM images of the TGA residues of the hybrid materials. The silica network morphology in the hybrid is clearly observed. Figure 10 shows that nanosized spherical silica particles were formed in the hybrids prepared in this work. It is clear that the average particle size increase with the modification circle though some extremely fine particles (<20 nm) also exist with silica load of 11.0%. This indicates that some subsequent impregnated silica coated on the silica core existed in PP matrix and others formed new particles. Figure 11 shows the EDAX elemental mapping of the TGA residual from hybrid containing 11.0% silica. The results shows that the stoichiometric ratio of silicon and oxygen is Si/O > 3. This indicates that not only silica but also other silicon compounds were present after the sol−gel process.[50] This is in line with the FTIR and ^{29}Si solid-state NMR observations. The presence of Pt is from the Pt coating used for SEM sample preparation.

TEM and SEM were also used to observe the morphology and microstructure of the hybrid. Figure 12a shows the TEM micrograph of the hybrid with 11.0% silica. The dark area on the micrograph shows irregular spherical silica nanoparticles. It is obvious that the size of most silica particles is in the range of 20−60 nm, which agree well with the SEM results. Parts b and c of Figure 12 are SEM images of the fracture surfaces

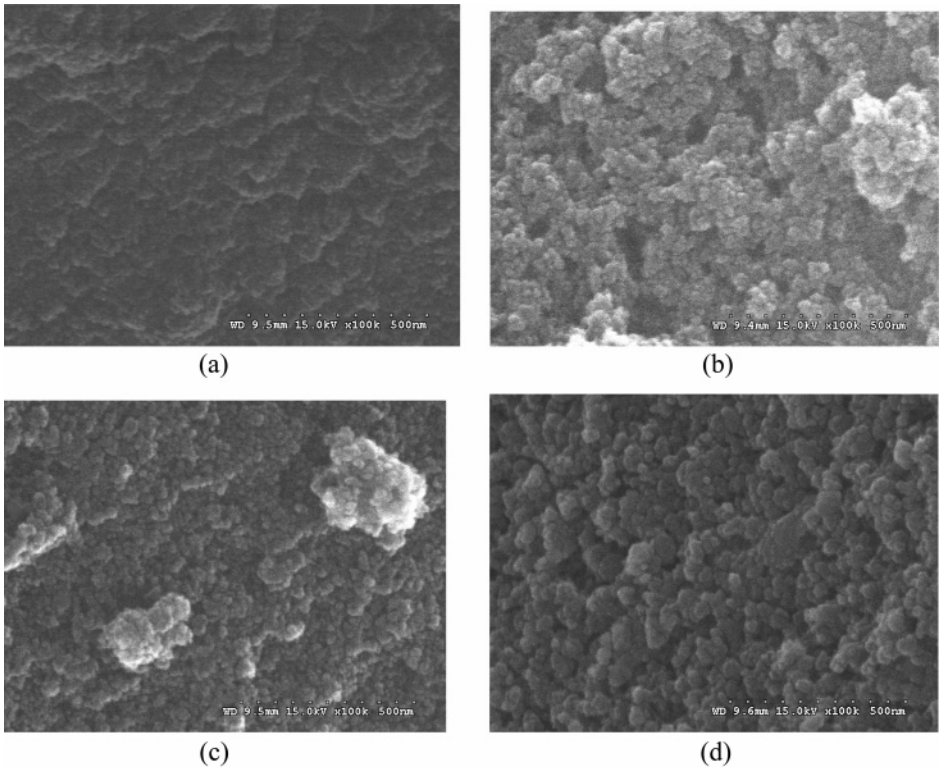

Figure 10. SEM images of the silica network from the TGA residues of the hybrids obtained at 600 °C. Silica contents in hybrid are (a) 1.9%, (b) 4.7%, (c) 8.5%, and (d) 11.0%.

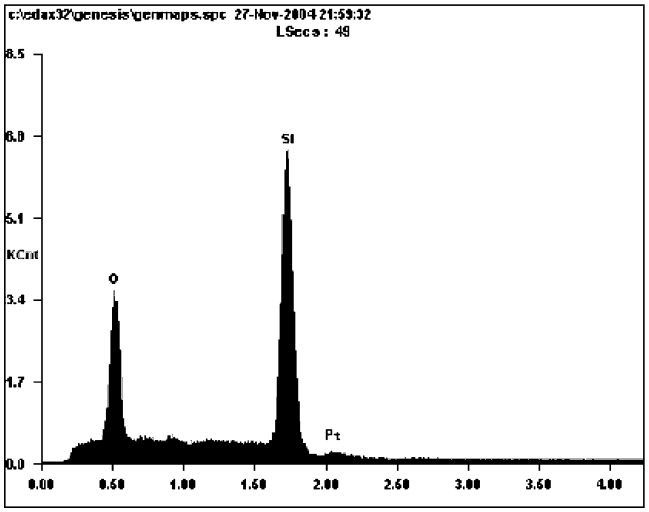

Figure 11. EDAX of the TGA residue from the composite containing 11.0% silica.

of the pure PP and the composite with 11.0% silica, respectively. The smooth surface of PP suggests the brittle break of PP in liquid N_2. The break surface morphology of the PP/silica composites is quite different from that of the pure PP. The spherical silica particles can be seen in Figure 12c and were uniformly distributed in the matrix. It can be clearly seen that these particles are tightly bonded to the matrix, indicating the strong interaction between organic polymers and silica particles. It should be noted that silica particles are not compatible with polyolefins. When used to blend with polyolefins by conventional methods, SiO_2 particles must be organically modified to partially prevent phase separation. However, in our system, the phase boundary between PP and silica is ambiguous, as shown in Figure 12a, and no obvious phase separation is observed. Furthermore, strong interaction between PP and silica particles can be deduced from the morphology of the fracture surface of the composite. This unusual phenomenon comes from the advantageous procedures of this work. The inorganic precursor, TEOS, was first uniformly deposited into PP matrix using SC CO_2. Subsequent hydrolysis and condensation result in the formation of inorganic silica network. With progress of condensation, it is reasonable to speculate that the silica network tends to separate from the organic phase due to their incompatibility. However, the macroscopic phase separation can be effectively prevented by the confinement of the silica in the organic matrix. In addition, in the present work, TEOS was first impregnated into and molecularly distributed in the amorphous region of PP. With the hydrolysis and condensation of the TEOS surrounding PP, silica networks were generated in-situ with some PP chains penetrating the three-dimensional networks. That is to say, local semiinterpenetrating polymer network (semi-IPN) structure was formed in this process. This unique microstructure may account for the significant increase of tensile properties as discussed below.

Tensile tests were used to evaluate the mechanical properties of the resultant materials. Corresponding stress−strain curves (Figure 13) show that all hybrids have typical characteristic of ductile materials. All samples undergo Hookean region, yield point, necking, neck extension, and ultimate break at higher module. It has been documented that hybrid polymeric materials with inorganic nanoparticles interconnected with each other over large distance turn to be brittle due to the high rigidity of the inorganic contiguous phase.[52] The tensile tests of our samples show that the silica particles are dispersed in the PP matrix separately, and the silica content is beneath its percolation threshold load. This is in line with the TEM and SEM results. It is clear the

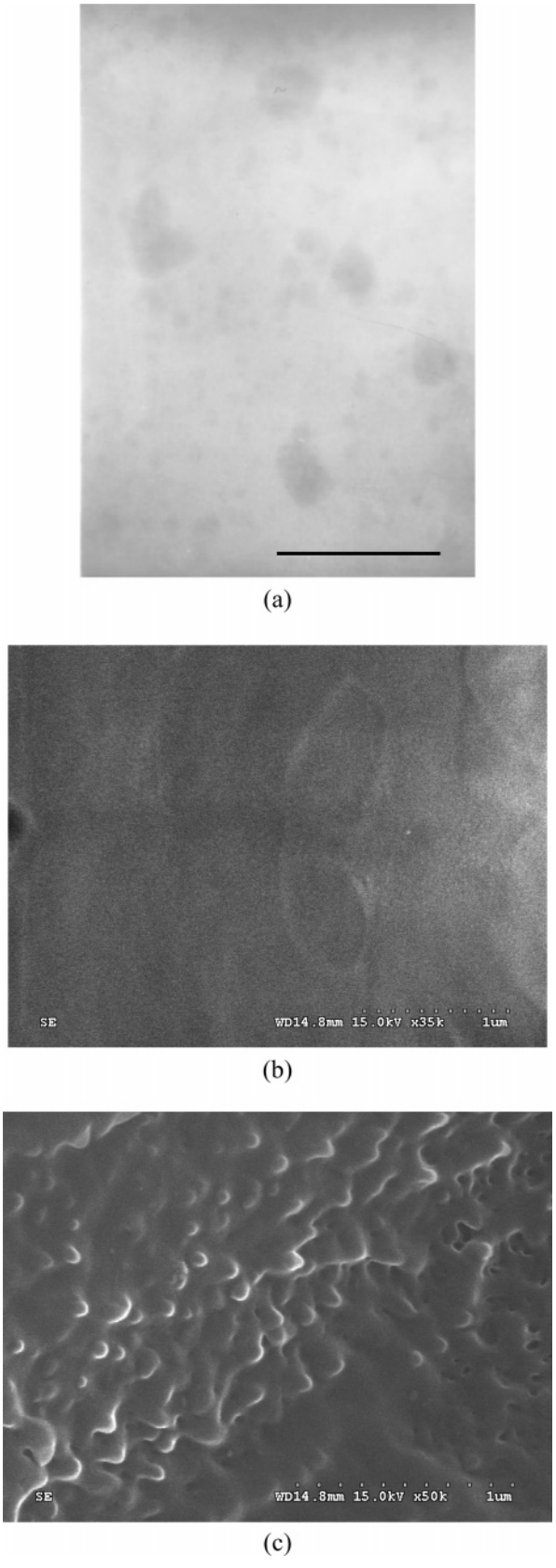

Figure 12. (a) TEM micrograph of the hybrid with silica content of 11.0%. The scale bar corresponds to 200 nm, (b) SEM micrograph of fracture surface of virgin PP, and (c) fracture surface of the composite with 11.0% silica.

elongation-at-break decrease with silica loading. The Young's modulus and tensile strength at yield point derived from Figure 13 are plotted in Figures 14 and 15. Significant increases in Young's modulus and tensile strength relative to the virgin PP are achieved. For example, more than 240% increases in the Young's modulus (714 vs 1710 MPa) and 160% increases in the tensile strength (22.7 vs 37.0 MPa) are observed for samples with 11.0 wt % silica. The only reported composite to achieve such a significant improvement in the Young's modulus was the polymer−clay nanocom-

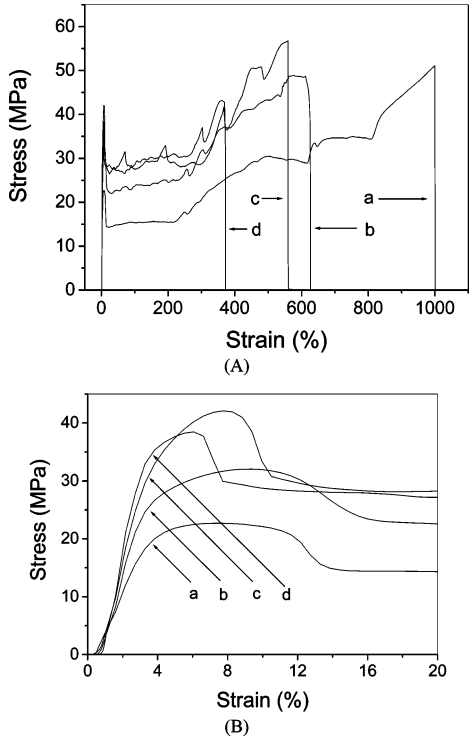

Figure 13. (A) Stress−strain curves of the hybrids with different silica contents. (B) Magnification of the curves with strain less than 20%. Silica contents of the samples are (a) 0, (b) 1.9%, (c) 8.5%, and (d) 11.0%.

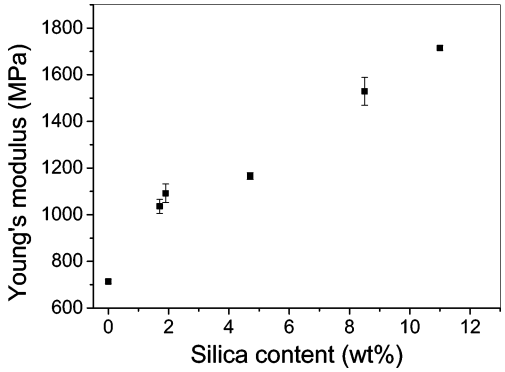

Figure 14. Young's modulus as a function of silica content.

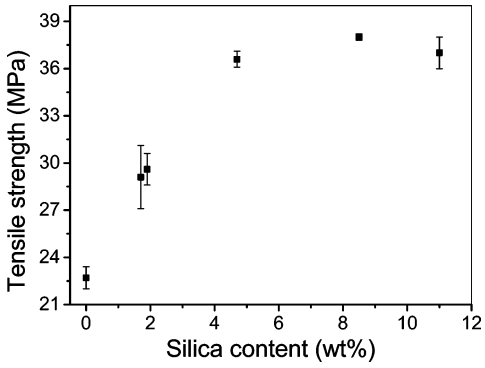

Figure 15. Tensile strength as a function of silica content.

posites prepared by in-situ polymerization with metallocene/clay catalysts.[13] The composite sample was subjected to DSC analysis to detect the crystallinity change during the impregnation and acidic water treatment. The crystallinity of the PP in the composite was 45.6%, which is nearly the same as that of the virgin PP films (44.5%). This suggests that the impregnation and heating in acidic water do not affect the crystallinity of the PP at our experimental conditions. Therefore, the significant increase is ascribed to the microstructure of the composites as mentioned above. As silica particles and PP matrix formed local semi-IPN structure in the amorphous region, the forced compatibility generates strong interaction between organic polymer and inorganic particles (as indicated in Figure 12c). Therefore, the three-dimensional networks may serve as rigid framework to improve the mechanical strength and modulus.

Conclusion

Polypropylene/silica hybrids can be prepared with the aid of SC CO_2. In this method TEOS is first impregnated into the PP matrix using SC CO_2 as a swelling agent and carrier. Subsequent treatment in acidic water at 80 °C induces the hydrolysis/condensation reaction of TEOS confined in PP network. The mass uptake of TEOS in the matrix can be tuned by changing temperature, CO_2 density, soaking time, and concentration of TEOS in the fluid phase during the soaking process. Hybrids with high silica loading can be easily obtained by repeating the impregnation and hydrolysis/condensation reaction steps. The formation of a three-dimensional silica network is confirmed by ATR-IR and solid-state ^{29}Si NMR. The hybrids show unusual microstructure, such as fine silica nanoparticles distributed uniformly in PP matrix, and no macroscopic phase separation can be observed in the hybrids, and the polymer molecules may entangle with the silica network. Significant increases in Young's modulus and tensile strength relative to the virgin PP are achieved. For example, more than 240% increases in the Young's modulus and 160% increases in the tensile strength are achieved for sample with 11.0 wt % silica. The impregnation/hydrolysis method present here represents a straightforward and effective way to prepare polymer/silica hybrid materials. It has special advantages for the polymers insoluble in common organic solvents and for preparing the composites in which the compatibility between the polymer and silica is poor.

Acknowledgment. The authors are grateful to the National Natural Science Foundation of China for financial support (20373080 20374057).

References and Notes

(1) Special issues of nanostructured materials. *Chem. Mater.* **1996**, *8*.
(2) Beecroft, L. L.; Ober, C. K. *Chem. Mater.* **1997**, *9*, 1302−1317.
(3) Innocenzi, P.; Brusatin, G. *Chem. Mater.* **2001**, *13*, 3126−3139.
(4) Usuki, A.; Kojima, Y.; Kawasumi, M.; Okada, A.; Fukushima, Y.; Jurauchi, T.; Kamigaito, O. *J. Mater. Res.* **1993**, *8*, 1179−1184.
(5) Kojima, Y.; Isilo, A.; Kawasumi, M.; Okada, A.; Fukushima, Y.; Kuarauchi, T.; Kamigaito, O. *J. Mater. Res.* **1993**, *8*, 1185−1191.
(6) Kawasumi, M.; Hasegawa, N.; Kato, M.; Usuki, A.; Okada, A. *Macromolecules* **1997**, *30*, 6333−6338.
(7) Galgali, G.; Ramesh, C.; Lele, A. *Macromolecules* **2001**, *34*, 852−858.
(8) Gopakumar, T. G.; Lee, J. A.; Kontopoulou, M.; Parent, J. S. *Polymer* **2002**, *43*, 5483−5491.
(9) Usuki, A.; Kato, M.; Okada, A.; Kurauchi, T. *J. Appl. Polym. Sci.* **1997**, *63*, 137−139.
(10) Tudor, J.; Willingto, L.; O'Hare, D. *Chem. Commun.* **1997**, 2031−2032.
(11) Bergman, J.; Chen, H.; Giannelis, E. P.; Thomas, M. G.; Coates, G. W. *Chem. Commun.* **1999**, 2179−2180.
(12) Johnson, L. C.; Killian, M. K.; Brookhart, M. *J. Am. Chem. Soc.* **1996**, *118*, 267−268.
(13) Sun, T.; Garcøs, J. M. *Adv. Mater.* **2002**, *14*, 128−129.
(14) Heinemann, J.; Reichert, P.; Thomann, R.; Mulhaupt, R. *Macromol. Rapid Commun.* **1999**, *20*, 423−430.
(15) Brinker, C. J.; Scherer, G. W. *Sol-Gel Science, The Physics and Chemistry of Sol-Gel Processing*; Academic Press: San Diego, 1990.
(16) Mark, J. E.; Jiang, C. Y.; Tang, M.-Y. *Macromolecules* **1984**, *17*, 2613−2618.
(17) Huang, H. H.; Wilkes, G. L. *Polym. Bull. (Berlin)* **1987**, *18*, 455−461.
(18) Landry, C. J. T.; Coltrain, B. K.; Brady, B. K. *Polymer* **1992**, *33*, 1486−1492.
(19) Kazarian, S. G. *J. Polym. Sci., Ser. C* **2000**, *42*, 78−101.
(20) Cooper, A. I. *J. Mater. Chem.* **2000**, *10*, 207−234.
(21) Cooper, A. I. *Adv. Mater.* **2001**, *13*, 1111−1114.
(22) Woods, H. M.; Silva, MMCG.; Nouvel, C.; Shakesheff, K. M.; Howdle, S. M. *J. Mater. Chem.* **2004**, *14*, 1663−1678.
(23) Tomasko, D. L.; Li, H. B.; Liu, D. H.; Han, X. M.; Wingert, M. J.; Lee, L. J.; Koelling, K. W. *Ind. Eng. Chem. Res.* **2003**, *42*, 6431−6456.
(24) Watkins, J. J.; McCarthy, T. J. *Macromolecules* **1994**, *27*, 4845−4847.
(25) Watkins, J. J.; McCarthy, T. J. *Macromolecules* **1995**, *28*, 4067−4074.
(26) Kung, E.; Lesser, A. J.; McCarthy, T. J. *Macromolecules* **1998**, *31*, 4160−4169.
(27) Arora, K. A.; Lesser, A. J.; McCarthy, T. J. *Macromolecules* **1999**, *32*, 2562−2568.
(28) Kung, E.; Lesser, A. J.; McCarthy, T. J. *Macromolecules* **2000**, *33*, 8192−8199.
(29) Muth, O.; Hirth, T. H.; Vogel, H. *J. Supercrit. Fluids* **2000**, *17*, 65−72.
(30) Zhang, J.; Busby, A. J.; Roberts, C. J.; Chen, X.; Davies, M. C.; Tendler, S. J. B.; Howdle, S. M. *Macromolecules* **2002**, *35,* 8869−8877.
(31) Li, D.; Han, B. *Ind. Eng. Chem. Res.* **2000**, *39*, 4506−4509.
(32) Liu, Z.; Dong, Z.; Han, B.; Wang, J.; He, J.; Yang, G. *Chem. Mater.* **2002**, *14*, 4619−4621.
(33) Li, D.; Liu, Z.; Han, B.; Song, L.; Yang, G.; Jiang, T. *Polymer* **2002**, *43*, 5363−5367.
(34) Li, D.; Han, B.; Liu, Z.; Zhao, D. *Polymer* **2001**, *42*, 2331−2337.
(35) Li, D.; Han, B.; Liu, Z. *Macromol. Chem. Phy.* **2001**, *202*, 2187−2194.
(36) Hayes, H. J.; McCarthy, T. J. *Macromolecules* **1998**, *31*, 4813−4819.
(37) Friedmann, G.; Guilbert, Y.; Catala, J. M. *Eur. Polym. J.* **2000**, *36*, 13−20.
(38) Spadaro, G.; De Gregorio, R.; Galia, A.; Valenza, A.; Filardo, G. *Polymer* **2000**, *41*, 3491−3494.
(39) Galia, A.; De Gregorio, R.; Spadaro, G.; Scialdone, O.; Filardo, G. *Macromolecules* **2004**, *37*, 4580−4589.
(40) Dong, Z.; Liu, Z.; Han, B.; He, J.; Jiang, T.; Yang, G. *J. Mater. Chem.* **2002**, *12*, 3565−3569.
(41) Sun, D.; Wang, B.; He, J.; Zhang, R.; Liu, Z.; Han, B.; Ying, H. *Polymer* **2004**, *45*, 3805−3810.
(42) Zerda, A. S.; Caskey, T. C.; Lesser, A. J. *Macromolecules* **2003**, *36*, 1603−1608.
(43) Green, J. W.; Rubal, M. J.; Osman, B. M.; Welsch, R. L.; Cassidy, P. E.; Fitch, J. W.; Blanda, M. T. *Polym. Adv. Technol.* **2000**, *11*, 820−825.
(44) Zeng, C.; Han, X.; Lee, L. J.; Koelling, K. W.; Tomasko, D. L. *Adv. Mater.* **2003**, *15*, 1743−1747.
(45) Bounor-Legaré, V.; Angelloz, C.; Blanc, P.; Cassagnau, P.; Michel, A. *Polymer* **2004**, *45*, 1485−1493.
(46) Colthup, N. B.; Daly, L. H.; Wiberley, S. E. *Introduction to Infrared and Raman spectroscopy*; Academic Press: London, 1975.
(47) Silverstein, R. M.; Bassler, G. C.; Morrill, T. C. *Spectrometric Identification of Organic* Compounds, 5th ed.; John Wiley & Sons: New York, 1991.

(48) Hsiue, G.-H.; Kuo, W.-J.; Huang, Y.-P.; Jeng, R.-J. *Polymer* **2000**, *14*, 2813−2825.
(49) Mauritz, K. A.; Warren, R. M. *Macromolecules* **1989**, *22*, 1730−1735.
(50) Gao, Y.; Choudhury, N. R.; Dutta, N.; Matisons, J.; Reading, M.; Delmotte, L. *Chem. Mater.* **2001**, *13*, 3644−3652.
(51) Siudak, D. A.; Start, P. R.; Mauritz, K. A. *J. Appl. Polym. Sci.* **2000**, *77*, 2832−2844.
(52) Shao, P. L.; Mauritz, K. A.; Moore, R. B. *Chem. Mater.* **1995**, *7*, 192−200.

MA047314H